

INTRODUCTION

Conjunctivitis is a common condition that significantly impacts quality of life due to recurrent irritations and uncomfortable symptoms resistance (Kammrath *et al.*, 2021; Gupta *et al.*, 2023). Any pathogenic organism capable of reaching the eye can cause inflammation, potentially affecting one or both eyes. Infections range from conjunctivitis, which is limited to the outer layer of the eye and the inner surface of the eyelid, to more serious conditions that affect visual acuity, such as keratoconjunctivitis and endophthalmitis, which can cause blindness (Taha *et al.* 2024). Viral conjunctivitis accounts for approximately 70% of all cases, and 30% of these are of bacterial origin (Al-Eryani, 2021).

In general, viral infections are more commonly seen in the acute phase of conjunctivitis. Bacterial conjunctivitis is most often caused by *Haemophilus aegyptius*, *Neisseria gonorrhoeae*, *Neisseria meningitidis*, *Corynebacterium xerosis*, and *Acinetobacter calcoaceticus* in newborns. The main cause is bacterial transmission from the mother during childbirth, where these strains are pathogenic to both mother and infant. Common bacteria in neonatal intensive care units include *Staphylococcus aureus*, *Streptococcus pyogenes*, and *Streptococcus faecalis*, while *Aerobacter* is most common in premature infants. (Voinescu *et al.*, 2025). The genus *Brachybacterium* was first discovered and recognized by scientists (Colliens *et al.*, 1988). These bacteria are non-motile, facultatively anaerobic or aerobic, Gram-positive, and do not produce spores. Cells of different species of *Brachybacterium* are spherical during the stationary phase and rod-shaped during the exponential phase (Ziganshina *et al.*, 2018).

Domain: Bacteria

Phylum: Actinobacteria

Class: Actinobacteria

Order: Micrococcales

Family: Dermabacteraceae

Genus: *Brachybacterium*

Species: *Brachybacterium epidermidis*

This classification came after taxonomic studies conducted on some *Brachybacterium* was proposed as a new genus by scientists since *Brevibacterium* species did not suit the traits of that genus. There are now 25 species with accurate and recorded names. It can be isolated from various environmental sources, such as seawater, plant roots and branches, rivers, cheese surfaces, coastal sand, and soil. Few studies have reported its isolation from human samples (Wu *et al.*, 2023). Species of this genus are ubiquitous and have been previously isolated from various sources, such as dogs, laboratory mice, insects, reptiles, fermented foods, poultry droppings, feces, and environmental samples (Hlaing *et al.*, 2019). In 2003, *Brachybacterium muris* was initially identified from a lab mouse's liver (Buczolits *et al.*, 2003), and was subsequently cut off from China's Chaka Salt Lake in 2017 (Gu *et al.*, 2017).

Additionally, it has been discovered in human nasal canals and skin (Leung *et al.*, 2020). A pleural effusion patient was found to have contracted *Brachybacterium muris* (We *et al.* 2023), it has also been isolated from a range of clinical specimens, including abscesses in the brain. (Bavbek *et al.*, 1998), cultures of blood (Gómez Garcés *et al.*, 2001), peritoneal fluid (Radtke *et al.*, 2001) and fatal septicemia (Lee *et al.*, 2011). It is regarded as an opportunistic pathogen as a result. (Tak *et al.*, 2018). Diagnoses at the species level are helpful in elucidating the pathogenic characteristics of *Brachybacterium* species that have been isolated from the human bloodstream. (Tamai *et al.*, 2018). A healthy 67-year-old woman's right hand was found to harbor a novel bacterium species called *B. epidermidis* (strain Marseille-Q2903) as part of a study that used cutting-edge bacterial culturing techniques to investigate the human microbiome. (Boxberger *et al.*, 2022).

G. mellonella larvae, also referred to as the "great wax moth," have become a substitute model organism in infectious illness research in recent years, especially for examining internal bacteria and

assessing the efficacy of medications. Due to the numerous benefits these larvae offer over vertebrate animal models, interest in them is expanding. They can be cultivated at 37°C, which is a temperature that many human pathogens can grow at, and practically speaking, they do not require expensive laboratory equipment. (Asai *et al.*, 2023). Also, the immune system of *G. mellonella* is functionally extremely similar to vertebrate systems. It is made up of humoral reactions, which include the release of antimicrobial peptides and defensive enzymes like prophenol oxidase, which uses myelination to detect infection, as well as blood cells (such leukocytes) that carry out phagocytosis. (Browne *et al.*, 2013; Hillyer, 2016).

This model's speed of infection and visual monitoring of illness progression through limited mobility or blackening of the larvae's body are noteworthy features. (Li *et al.*, 2018).

Additionally, research has demonstrated that some bacterial strains pathogenicity in *G. mellonella* larvae is frequently comparable to that seen in mammalian models, which makes this model highly helpful for evaluating the early effectiveness of medications prior to doing animal or human trials (Tsai *et al.*, 2016; Dinh *et al.*, 2021). Moreover, the application of *G. mellonella* is consistent with the worldwide movement to lessen the dependence on vertebrates in scientific research, and the *G. mellonella* model is becoming a more significant and ethical tool for acquiring crucial and trustworthy primary data. (Ménard *et al.*, 2021).

MATERIALS AND METHODS

At Mosul General Hospital, Ibn Al-Atheer Hospital, and Al-Salam Teaching Hospital, 100 conjunctival swab samples were taken from newborns with conjunctivitis. The swabs were cultured on blood agar, chocolate agar, MacConkey agar, and mannitol salt agar. They were incubated at 37°C for 24-48 hours using a candle jar and using catalase & oxidase tests were performed to identify the bacterial isolates under study (Bauman, 2018).

Molecular Diagnosis

DNA extraction was performed using the Geneaid extraction kit. To determine the sequence of the isolates under study, universal primers for the *16S rRNA* gene were used, as shown in (Table 1).

These primers were obtained from American company Promega. Each primer was dissolved in deionized water to serve as a stock solution at a final concentration of 100 pmol/μL. and the total PCR reaction is 25 μL as shown in (Table 2). (Al-najim; Alsammak., 2024) (Al-jarjary and Alsammak, 2024)

Table (1): universal primers for determining the sequences *16S rRNA*

Gene	Primer	Sequence	Reference
16S rRNA	27F	5'-AGAGTTTGGATCTGGCTCAG-3'	(Salih <i>et al.</i> , 2019)
	1492R	5'-CGGTTACCTTGTTACGACTT-3'	

Table (2): PCR reaction Mixture

No.	Component	Size in μL
1.	Master Mix	12.5
2.	Forward primer	1.5
3.	Reverse primer	1.5
4.	Dd H2O	5.5
5.	DNA template	4
	Total size	25

DNA amplification, according to the program shown in (Table 3).

Table (3): PCR conditions for amplification the gene of 16S rRNA

Steps	Temp.	Time	Cycles
Initial denaturation	95 °C	5 min	1
Denaturation	95 °C	30 sec	30
Annealing	55 °C	30 sec	30
Extension	72 °C	1 min	30
Final extension	72 °C	3 min	3

One hundred base pair DNA ladder was used to estimate the sizes of PCR products, and it was loaded into the first well of the agarose gel. After the gel was fully prepared, it was submerged in 1x TBE running buffer, and electrophoresis was initiated at 12 volts, gradually increasing to 65 volts for one hour. The gel was examined under ultraviolet (UV) light at a wavelength of 320 nm.

Pathogenicity test on *Galleria mellonella* larvae

1. Last instar larvae of *G. mellonella* were collected from the College of Agriculture, University of Mosul. Selected larvae weighed between 200 and 250 mg and measured 1.5-2.5 cm in length. Only light-colored larvae without dark spots or pigmentation were used.
2. Larvae were placed in Petri dishes and maintained at 37°C for experimentation.
3. For bacterial inoculum preparation, 5 mL of nutrient broth was used culture, incubated for 18-24 hours. Bacterial Cultures were centrifuged at room temperature at 6000 rpm for 7 minutes.
4. The supernatant was discarded, and the pellet was resuspended in 1 mL of phosphate-buffered saline (PBS). The bacterial suspension was then diluted in PBS to an OD600nm equivalent to approximately 1×10^9 CFU/mL.
5. Using an insulin syringe, 10 μ L of the diluted bacterial suspension was injected into the second last left proleg of each larva (three larvae per group) after disinfecting the injection site with 70% ethanol. To confirm that the injection procedure did not itself cause mortality, a control group of three larvae was injected with 10 μ L of sterile PBS. All larvae were incubated in the dark at 37°C for 24 to 72 hours.
6. The larvae were observed to change color from light brown to dark brown, then black, and were considered dead when touched (Andrea *et al.*, 2019).

Histological studies:

Dead larvae injected with bacteria and control larvae were preserved in a 10% formalin solution. The preserved larvae were sent to the College of Veterinary Medicine, University of Mosul, for histological examination according to the method (Emery *et al.*, 2019). Before immersing them in wax, the larvae were divided into segments: the head, the midgut, and the posterior (anal) segment, and preserved in 70% ethanol. Samples were dried using series concentrations of ethanol (70%, 80%, and 90%) for one hour for each sample. The samples were then washed three times in 100% ethanol for one hour each to remove any residual traces. The dried samples were washed twice in HistoClear for one hour before being fully immersed in wax. The samples were then resuspended in paraffin wax for one hour. A microtome was used to cut the embedded samples into 6-micrometer-thick slices, which were then fixed on glass slides using egg albumin (1% w/v) and left to dry for 24 hours before staining. Hematoxylin and eosin staining was used to stain the mounted slides.

RESULTS AND DISCUSSION

One *B. epidermidis* isolate was identified from a total of 100 samples. the colonies appeared as small yellow to green, and the cells were spherical under the microscope, Fig. (1: A, B). They were catalase-positive and oxidase-negative. The isolation bacteria are

44% and 2.27% one strain *B. epidermidis* rate was 2.27% as Fig. (2) of the total 100 pathological samples.

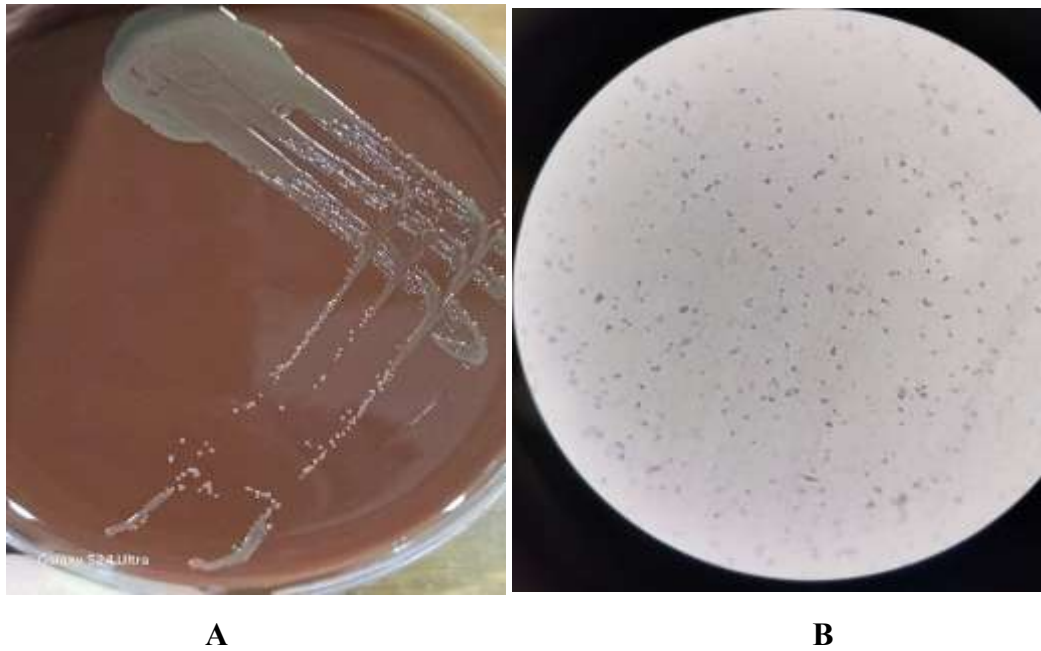


Fig. 1: *Brachy bacterium epidermidis* in A chocolate ager and B the cells under microscopic at 100x.

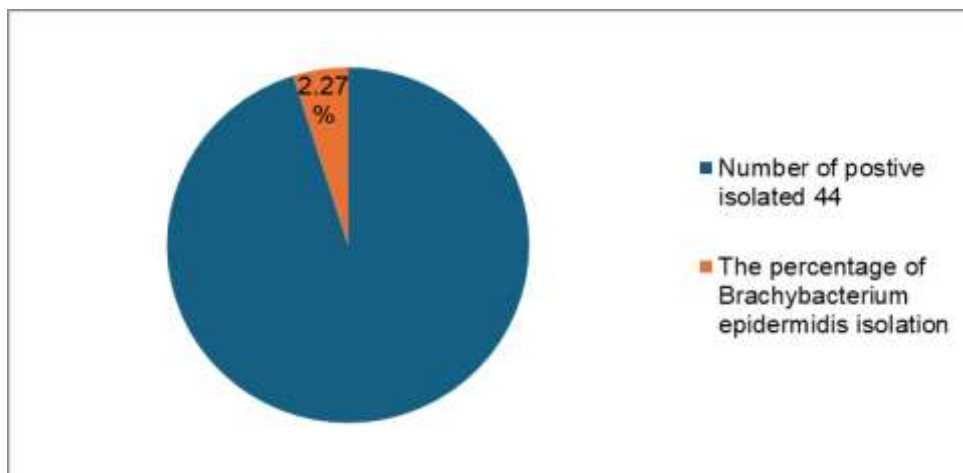


Fig. 2: The percentage of *Brachy bacterium epidermidis* isolation

The universal primer *16S rRNA* was used for molecular identification of the isolate, as bands appeared in comparison with the ladder, as shown in Fig. (3)

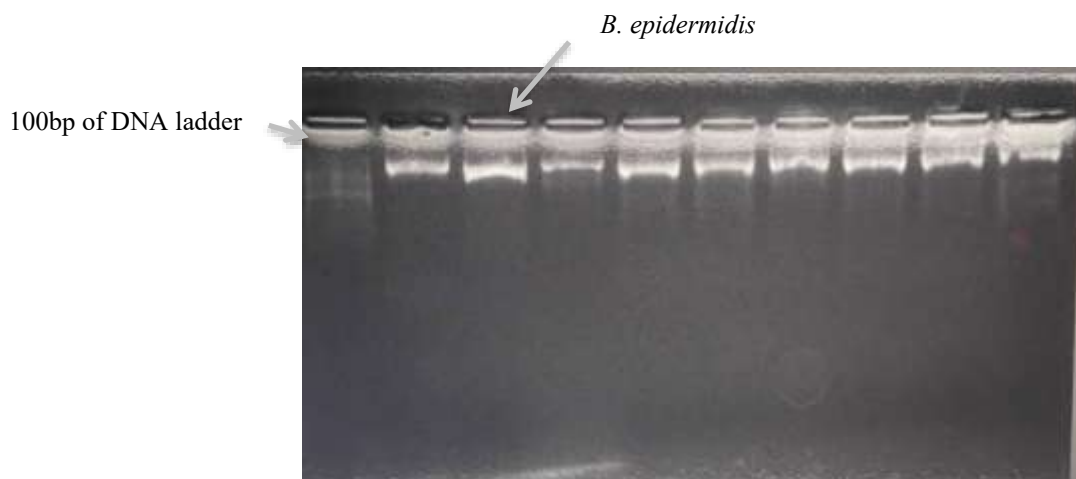


Fig. 3: Amplification of the 16S rRNA gene

The obtained sequence of the isolate was compared with reference sequences using the Basic Local Alignment Search Tool (BLAST) available on the NCBI database. The results confirmed that the isolate belongs to *B. epidermidis*, showing a similarity range of 96-100% with the reference strain. Following the injection of *B. epidermidis* into *G. mellonella* larvae, phenotypic changes were observed. The larvae changed in color from light brown to dark brown and eventually to black within 24 hours. In contrast, the control larvae remained active and maintained their normal coloration, as shown in Fig. (4)



Fig. 4: The difference between infected *Galleria mellonella* larvae and the control larvae.

Histological results on *G. mellonella* larvae revealed the effects of infection with *B. epidermidis* bacteria, demonstrating clear changes in infected larvae compared to control larvae.

Histological sections of uninfected larvae showed the integrity of various tissues, such as the skin, skeletal muscles, silk glands, adipose tissue, respiratory system, and gastrointestinal tract, indicating absence of pathological alterations and the absence of any signs of inflammation or necrosis Fig. (5), Fig. (6) and Fig. (7).



Fig. 5: Transverse histological section of the *Galleria mellonella* larvae of the control group shows the intact histology of the cuticle (Cu), skeletal muscles (SM), silk glands (SG) and fat tissue (FT). Hematoxylin & Eosin stain, 40X, Scale bar=100μm.

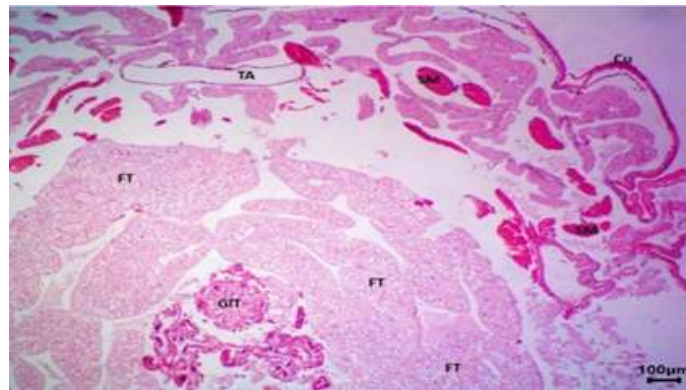


Figure 6: Transverse histological section of the *Galleria mellonella* larvae of the control group shows the intact histology of the cuticle (Cu), skeletal muscles (SM), tracheal apparatus (TA), gastrointestinal tract (GIT) and fat tissue (FT). Hematoxylin & Eosin stain, 40X, Scale bar=100μm.

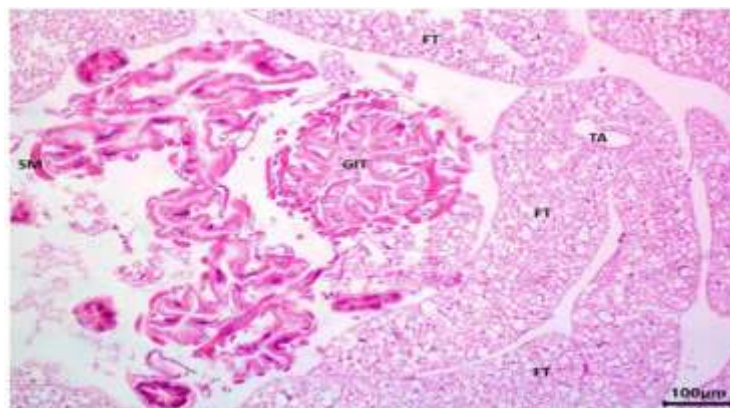


Figure 7: Transverse histological section of the *Galleria mellonella* larvae of the control group shows the intact histology of the cuticle (Cu), skeletal muscles (SM), tracheal apparatus (TA), gastrointestinal tract (GIT) and fat tissue (FT). Hematoxylin & Eosin stain, 100X, Scale bar=100μm.

In contrast, larvae infected with *B. epidermidis* exhibited multiple pathological histological signs, including:

1. Disruption and rupture of the cuticle, which may indicate degradation of the larval protective barrier due to enzymatic activity or bacterial toxicity.

2. Dense aggregations of hemocytes, representing an early immune response to the infection.
3. A noticeable increase in proteinaceous fluid, which may be associated with enhanced vascular permeability or cellular death.
4. Gastrointestinal tract necrosis and epithelium shrinkage are clear signs of infection-induced cellular damage.
5. Deterioration of the structure of the muscle fibers combined with skeletal muscle necrosis.
6. Melanized nodules, a recognized immunological signature that encapsulates pathogenic pathogens, are seen in *G. mellonella* (Browne *et al.*, 2013).

These histological alterations, which include nodule formation, melanin synthesis, and arterial phagocytosis, are a definite sign of *G. mellonella* typical immunological response (Tsai *et al.*, 2016). These findings align with those published in research by (Tsai *et al.* 2016). It showed how bacterial infections in *G. mellonella* can seriously harm tissue, particularly when very aggressive bacterial strains are used.

A recent study by Asai *et al.* 2023, supports the use of as a substitute model for researching bacterial virulence and immunological tests since it has a widely recognized immune response that is comparable to that of mammals. The same study was released by Iwański *et al.* 2023, noticed comparable histological alterations, such as pigment nodules, muscle tissue necrosis, and structural degradation, in *Pseudomonas aeruginosa* infections. The mechanism of action of *Shigella* bacteria on *G. mellonella* larvae was studied. The results showed that mortality rates depended on the type of strain and the dose of infection. Melanin pigmentation was also shown to be a common indicator of larval response to stress or infection, as this response causes the larvae to change color from their normal cream color to dark brown or black. Experiments showed that high concentrations of bacteria spread rapidly within the larvae compared to low concentrations, causing a clear change in the larval appearance, indicating the severity of the disease reaction, as a show in (fig from 8 to 12) (Barnoy *et al.*, 2017).

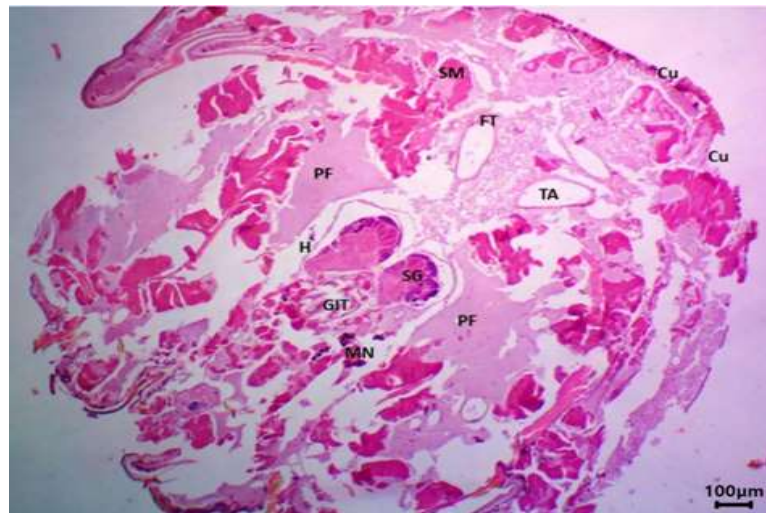


Fig. 8: Transverse histological section of the *Galleria mellonella* larvae of the bacterial infected group shows the interruption of the cuticle (Cu), presence of silk glands (SG), aggregates of hemocytes (H), increase proteinaceous fluid (PF) necrosis in gastrointestinal tract (GI), necrosis in the skeletal muscles (SM), and presence of melanized nodule (MN). Hematoxylin & Eosin stain, 40X, Scale bar=100µm.

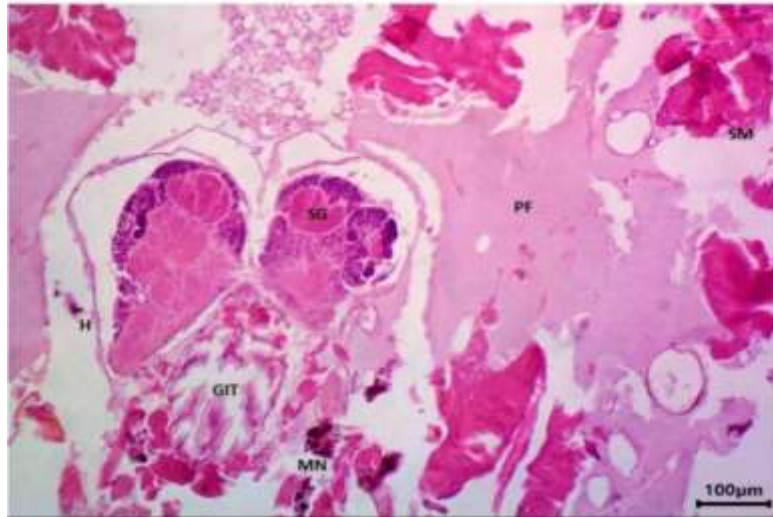


Fig. 9: Transverse histological section of the *Galleria mellonella* larvae of the bacterial infected group shows the interruption of the cuticle (Cu), presence of silk glands (SG), aggregates of hemocytes (H), increase proteinaceous fluid (PF) necrosis in gastrointestinal tract (GI) with shortened of epithelium (arrows) necrosis in the skeletal muscles (SM), and presence of melanized nodule (MN). Hematoxylin & Eosin stain, 100X, Scale bar=100µm.

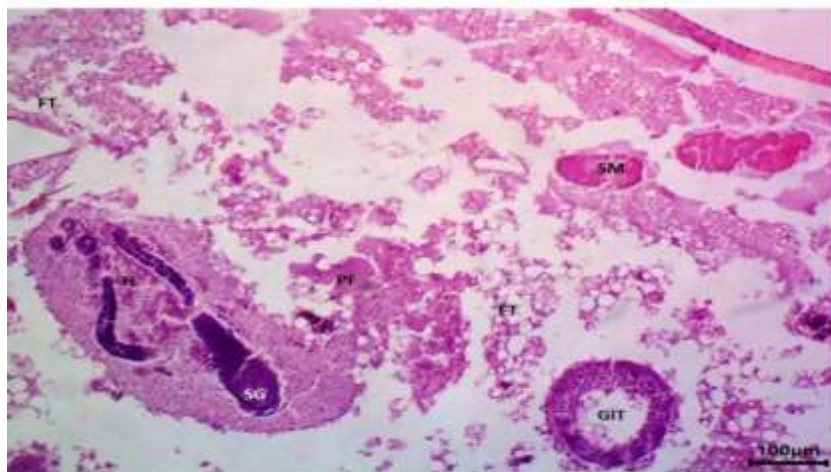


Fig. 10: Transverse histological section of the *Galleria mellonella* larvae of the bacterial infected group shows the interruption and loss of the fat tissue (FT), presence of silk glands (SG), aggregates of hemocytes (H), increase proteinaceous fluid (PF) necrosis in gastrointestinal tract (GI), necrosis in the skeletal muscles (SM). Hematoxylin & Eosin stain, 40X, Scale bar=100µm.

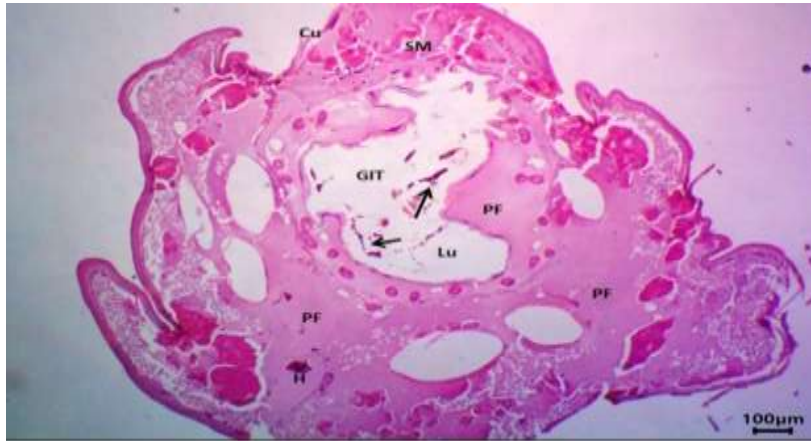


Fig. 11: Transverse histological section of the *Galleria mellonella* larvae of the bacterial infected group shows the interruption and loss of the cuticle (Cu), aggregates of hemocytes (H), increase proteinaceous fluid (PF) necrosis in gastrointestinal tract (GI) with sloughing of the epithelial cells (arrows) in the lumen (Lu), and necrosis in the skeletal muscles (SM). Hematoxylin & Eosin stain, 40X, Scale bar=100µm.

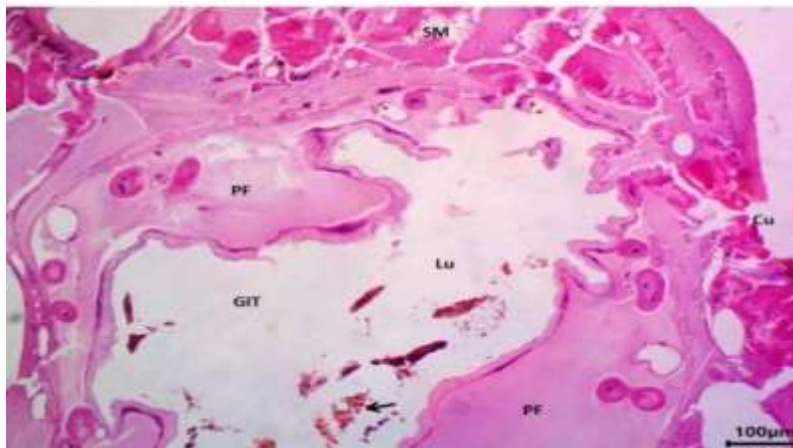


Figure 12: Transverse histological section of the *Galleria mellonella* larvae of the bacterial infected group shows the interruption and loss of the cuticle (Cu), increase proteinaceous fluid (PF) necrosis in gastrointestinal tract (GI) with sloughing of the epithelial cells (arrows) in the lumen (Lu), and necrosis in the skeletal muscles (SM). Hematoxylin & Eosin stain, 100X, Scale bar=100µm

CONCLUSIONS

B. epidermidis isolated for the first time in Iraq from a case of neonatal conjunctivitis and reported for only the second time worldwide, induced histopathological alterations in the larvae of demonstrated a clear ability to induce significant pathological effects in the tissues of *G. mellonella* larvae.

These results represent an important scientific addition, as they are among the few studies that shed light on the tissue-mediated effects of this bacterium on this model organism. This opens the door for further studies on the mechanisms of bacterial virulence and resistance using alternative vertebrate animal models.

REFERENCE

- Al Jarjary, H.; Alsammak, E. (2023). Phylogenetic analysis of *16S rRNA* gene of *Burkholderia cepacia* complex species isolated from different clinical sources. *Raf. J. Sci.*, **32**(3), 19-30. doi.org/10.33899/rjs.2023.180288
- Al-Eryani, S. A.; Alshamahi, E. Y. A.; Al-Shamahy, H. A.; Alfalahi, G. H. A.; Al-Rafiq, A. A. (2021). Bacterial conjunctivitis of adults: Causes and ophthalmic antibiotic resistance patterns for the common bacterial isolates. *Unive. J. Pharma. Rese.*, **6**(1). doi.org/10.22270/ujpr.v6i1.535
- Al-Najim, A. N. M.; Alsammak, E. G. (2024). Antibiofilm activity of Mersacidin produced by *Bacillus* sp.-AE against *Acinetobacter baumannii* and *Acinetobacter junii* isolated from clinical specimens. *Raf. J. Sci.*, 331928–1914. doi.org/10.33899/rjs.2024.183433
- Andrea, A.; Krogfelt, K. A.; Jenssen, H. (2019). Methods and challenges of using the greater wax moth (*Galleria mellonella*) as a model organism in antimicrobial compound discovery. *Micro.*, **7**(3), 85. doi.org/10.3390/microorganisms7030085
- Asai, M., Li, Y.; Newton, S. M.; Robertson, B. D.; Langford, P. R. (2023). *Galleria mellonella*-intracellular bacteria pathogen infection models: the ins and outs. *FEMS Microb. Rev.*, **47**(2), fuad011. doi.org/10.1093/femsre/fuad011
- Barnoy, S.; Gancz, H.; Zhu, Y.; Honnold, C. L.; Zurawski, D. V.; Venkatesan, M. M. (2017). The *Galleria mellonella* larvae as an in vivo model for evaluation of *Shigella* virulence. *Gut Microbes*, **8**(4), 335-350.
- Bauman, R. W. (2018). "Microbiology With Diseases by Body System" 5th ed. Pearson Education, Inc.
- Bavbek, M.; Caner, H.; Arslan, H.; Demirhan, B.; Tunçbilek, S; Altinörs, N. (1998). Cerebral *Dermabacter hominis* abscess. *Infection*, **26**(3), 181-183. doi.org/10.1007/BF02771848
- Boxberger, M.; Magnien, S.; Antezack, A.; Rolland, C.; Makoa, M.; La Scola, B.; Cassir, N. (2022). *Brachybacterium epidermidis* sp. nov., a novel bacterial species isolated from the back of the right hand, in a 67-year-old healthy woman. *Int. J. Microb.*, **8**. doi.org/10.1155/2022/2875994
- Browne, N.; Heelan, M.; Kavanagh, K. (2013). An analysis of the structural and functional similarities of insect hemocytes and mammalian phagocytes. *Viral.*, **4**(7), 597-603 doi.org/10.4161/viru.25906
- Buczolits, S.; Schumann, P.; Weidler, G.; Radax, C.; Busse, H. J. (2003). *Brachybacterium muris* sp. Nov., isolated from the liver of a laboratory mouse strain. *Int. J. Syst. Evol. Microb.*, **53**, 1955-1960.
- Collins, M. D.; Brown, J.; Jones, D. (1988). *Brachybacterium faecium* gen. Nov., sp. Nov., a coryneform bacterium from poultry deep litter. *Int. J. Syst. Bact.* **38**(1), 45-48.
- Dinh, H.; Semenec, L.; Kumar, S. S.; Short, F. L.; Cain, A. K. (2021). Microbiology's next top model: *Galleria* in the molecular age. *Pathog. Dise.*, **79**(2), ftab006. doi.org/10.1093/femspd/ftab006
- Emery, H.; Johnston, R.; Rowley, A. F.; Coates, C. J. (2019). Indomethacin-induced gut damage in a surrogate insect model, *Galleria mellonella*. *Arch. Toxicol.* **93**, 2347-2360. doi.org/10.1007/s00204-019-02506
- Gómez-Garcés, J. L.; Oteo, J.; García, G.; Aracil, B.; Alós, J. I.; Funke, G. (2001). Bacteremia by *Dermabacter hominis*, a rare pathogen. *J. Clin. Microbiol.*, **39**(6), 2356-2357. doi.org/10.1128/JCM.39.6.2356-2357.2001
- Gu, D.; Jiao, Y.; Wu, J.; Liu, Z.; Chen, Q. (2017). Optimization of EPS Production and Characterization by a Halophilic Bacterium, *Kocuria rosea* ZJUQH from Chaka Salt Lake with Response Surface Methodology. *Molecules*, **22**(5), 814. doi.org/10.3390/molecules22050814

- Gupta, S.; Rahman, M.; Tibrewal, S.; Gaur, A.; Ganesh, S.; Sangwan, V. S. (2023). Evaluation of dry eyes in children with vernal kerato-conjunctivitis using clinical tests and ocular surface analysis. *Indian J. Opth.*, **71**(4), 1488-1494. doi.org/10.4103/IJO.IJO_2836_22
- Hillyer, J. F. (2016). Insect immunology and hematopoiesis. *Dev. Comp. Immunol*, **58**, 102-118. doi.org/10.1016/j.dci.2015.12.006
- Hlaing, P. P. T.; Junqueira, A. C. M.; Uchida, A.; Purbojati, R. W.; Houghton, J. N. I.; Chénard, C., Wong, A.; Schuster, S. C. (2019). Complete genome sequence of *Brachybacterium* sp. strain SGAir0954, isolated from Singapore air. *Microbiol. Resour. Announc.*, **8**(23), 19-19. doi.org/10.1128/MRA.00619-19
- Iwański, B.; Mizerska-Kowalska, M.; Andrejko, M. (2023). Pseudomonas aeruginosa exotoxin A induces apoptosis in *Galleria mellonella* hemocytes. *J. Invert. Pathol.* **197**, 107884. doi.org/10.1016/j.jip.2023.107884
- Kammrath Betancor, P.; Tizek, L.; Zink, A.; Reinhard, T.; Böhringer, D. (2021). Estimating the Incidence of Conjunctivitis by Comparing the Frequency of Google Search Terms with Clinical Data: Retrospective Study. *JMIR public health Surveill.*, **7**(3), e22645. doi.org/10.2196/22645
- Lee, H. J.; Cho, C. H.; Kwon, M. J.; Nam, M. H.; Lee, K. N.; Lee, C. K. (2011). A patient with fatal septicemia caused by a rare pathogen *Dermabacter hominis*. *Infect. Chemother*, **43**(1), 86-88. doi.org/10.3947/ic.2011.43.1.86
- Leung, M. H. Y.; Tong, X.; Bastien, P.; (2020). Changes of the human skin microbiota upon chronic exposure to polycyclic aromatic hydrocarbon pollutants. *Microbi.*, **8**(1), 100. doi.org/10.1186/s40168-020-00874-1
- Li, Y.; Spiropoulos, J.; Cooley, W.; Khara, J. S.; Gladstone, C. A., Asai, M.; Langford, P. R. (2018). *Galleria mellonella*- a novel infection model for the *Mycobacterium tuberculosis* complex. *Virulence*, **9**(1), 1126-1137. doi.org/10.1080/21505594.2018
- Ménard, G.; Rouillon, A.; Cattoir, V.; Donnio, P. Y. (2021). *Galleria mellonella* as a suitable model of bacterial infection: Past, present and future. *Front. Cell. Infect. Microbiol.*, **11**, 782733. doi.org/10.3389/fcimb.2021.782733
- Radtke A.; Bergh K.; Øien CM.; Bevanger L.S. Peritoneal dialysis-associated peritonitis caused by *Dermabacter hominis* (2001). *J. clin. Microb.*, **39**(9), 3420-1. doi:10.1128/JCM.39.9.3420-3421.2001
- Taha, N. Y.; Nijris, O. N.; Salh, M. K. (2024). Isolation and identification of bacteria causing conjunctivitis. *Samarra J. Pure Appl. Sci.*, **6**(32), 86-97. doi.org/10.54153/sjpas.2024.v6i3(2).890
- Tak, E. J.; Kim, P. S.; Hyun, D. W.; Kim, H. S.; Lee, J. Y.; Kang, W.; Sung, H.; Shin, N. R.; Kim, M. S.; Whon, T. W.; Bae, J.W. (2018). Phenotypic and genomic properties of *Brachybacterium vulturis* sp. nov. and *Brachybacterium avium* sp. Nov. *Front. Microbiol.* **9**, 1809. doi.org/10.3389/fmicb.2018.01809
- Tamai, K.; Akashi, Y.; Yoshimoto, Y.; Yaguchi, Y.; Takeuchi, Y.; Shiigai, M.; Igarashi, J.; Hirose, Y.; Suzuki, H.; Ohkusu, K. (2018). First case of a bloodstream infection caused by the genus *Brachybacterium*. *J. Infet. Chemother.* doi.org/10.1016/j.jiac.2018.06.005
- Tsai, C. J. Y.; Loh, J. M. S.; Proft, T. (2016). *Galleria mellonella* infection models for the study of bacterial diseases and for antimicrobial drug testing. *Virulence*, **7**(3), 214-229. doi.org/10.1080/21505594.2015.1135289
- Voinescu, A.; Musuroi, C.; Licker, M., Muntean, D.; Musuroi, S.I.; Baditoiu, L. M.; Dugaesescu, D.; Jumanca, R.; Munteanu, M.; Cosnita, A. (2025). Comparative Analysis of Bacterial Conjunctivitis in the Adult and Pediatric Inpatient vs. Outpatient Population. *Microorgan.* **13**(3), 473. doi.org/10.3390/microorganisms13030473

- Wu, Y.; Wang, S.; Wu, G.; Zhang, J.; Liu, S. (2023). *Brachy bacterium muris* Detected in a Hepatocellular Carcinoma Patient with Pleural Effusion: A Case Report. *Infect. Drug Resist.* 16, 3003-3006. doi.org/10.2147/IDR.S406259
- Ziganshina, E. E.; Mohammed W. S.; Shagimardanova, E. I.; Ziganshi, A. M. (2018) Draft genome sequence data and analysis Of *Brachy bacterium sp.* Strain EE-P12 isolated from a laboratory-scale anaerobic ranalysis. *Data Brief.*, 21, 2576-2580. doi.org/10.1016/j.dib.2018.11.104

استخدام يرقة *Galleria mellonella* للتحري عن الضراوة المرضية لبكتريا

Brachy bacterium epidermidis المعزولة من التهاب ملتحمة العين لدى حديثي الولادة في مدينة الموصل

طبية نشوان سالم اسراء غانم السماك

قسم علوم الحياة/ كلية العلوم/ جامعة الموصل

ايمكا اوبراجي

قسم الكيمياء الحيوية التطبيقية/ جامعة ولاية العلوم الطبية والتطبيقية/ إغبو-إينو/ نيجيريا

الملخص

تم جمع 100 عينة سريرية من أطفال حديثي الولادة المصابين بالتهاب ملتحمة العين من ثلاثة مستشفيات في مدينة الموصل: مستشفى السلام التعليمي، مستشفى الموصل العام، ومستشفى ابن الأثير. أظهرت 44% من هذه العينات نمواً على الأوساط الزرعية، وكانت نسبة عزل بكتيريا *Brachy bacterium epidermidis* 2.27% وهي المرة الأولى التي يتم فيها عزل هذا النوع البكتيري من حالات التهاب الملتحمة في مدينة الموصل/العراق

وأظهرت *Brachy bacterium epidermidis* نمواً على وسط أكار الدم المطبوخ (Chocolate agar) ، وتم تشخيصها مظهرياً، ثم أُجري عليها التشخيص الجزيئي باستخدام البادئ العام *16S rRNA* تمت مقارنة نتائج تسلسل القواعد النوكلويدية للعزلة مع التسلسلات القياسية المثبتة في National Center for Biotechnology Information (NCBI) باستخدام أداة (BLAST (Basic Local Alignment Search Tool) ، وأكدت النتائج أن العزلة تعود إلى *Brachy bacterium epidermidis* إذ أظهرت نسبة تشابه 100% مع Marseille-Q2903.

ولغرض تقييم التأثير الحيوي لهذا النوع البكتيري *Brachy bacterium epidermidis* Marseille-Q2903، تم استخدام يرقات *Galleria mellonella*، حيث حُقنت مجموعة من اليرقات بمعلق بكتيري قياسي، في حين حُقنت مجموعة السيطرة بمحلول منظم. أظهرت اليرقات المصابة تغيرات مظهرية ونسجية واضحة مقارنة بمجموعة السيطرة، مما يشير إلى قدرة البكتيريا المعزولة على إحداث تأثيرات مرضية.

الكلمات الدالة: التهاب المخيخ، *Brachy bacterium*، *Galleria mellonella*، حديثي الولادة، الأمراض.